Electronic Supplementary Material (ESI) for Physical Chemistry Chemical Physics.

Supplementary Information

New insights into the origin of unstable sodium graphite intercalation compounds

Olena Lenchuk[a,b], *Philipp Adelhelm*[c], *Doreen Mollenhauer*[a,b]*

[a] Institute of Physical Chemistry, Justus-Liebig University Giessen, 35392 Giessen, Germany

[b] Center for Materials Research (LaMa), Justus-Liebig University Giessen, 35392 Giessen, Germany

[c] Institute of Technical Chemistry and Environmental Chemistry, CEEC Jena, Friedrich-Schiller University Jena, 07743 Jena, Germany

**E-Mail*: doreen.mollenhauer@phys.chemie.uni-giessen.de

A) Stability of alkali-metal graphite intercalation compounds

Table S1. The calculated formation energies (E_f in eV/f.u.) of AM-GICs (AM = Li, Na and K) for different AM concentrations.

Compound	Number of atoms in the supercell	E_f, eV/f.u.			Stage	Low-energy stacking
		AB-stacking	AA-stacking	AA-stacking*		
Li						
LiC_6	6 Li, 36 C	-0.054	-0.246	-0.299	I	AA
LiC_8	2 Li, 16 C	-0.032	-0.218	-0.290	I	AA
LiC_{12}	3 Li, 36 C	0.081	-0.058	-0.166	II	AA
LiC_{16}	1 Li, 36 C	0.043	-0.039	-0.182	II	AA
LiC_{32}	1 Li, 32 C	-0.008	0.005	-0.281	II	AB
LiC_{32}	1 Li, 32 C	0.000	0.093	-0.193	IV	AB
LiC_{36}	1 Li, 36C	-0.028	0.001	-0.321	II	AB
LiC_{64}	1 Li, 64C	-0.053	0.176	-0.397	II	AB
LiC_{72}	1 Li, 72 C	-0.078	0.239	-0.403	II	AB
LiC_{72}	1 Li, 72 C	-0.077	0.279	-0.362	IV	AB
Na						
NaC_6	6 Na, 36 C	0.193	0.061	0.007	I	AA
NaC_8	2 Na, 16 C	0.210	0.058	-0.014	I	AA
NaC_{12}	3 Na, 36 C	0.357	0.221	0.114	II	AA
NaC_{16}	1 Na, 36 C	0.252	0.189	0.046	II	AA
NaC_{32}	1 Na, 32 C	0.303	0.308	0.021	II	AB
NaC_{32}	1 Na, 32 C	0.213	0.303	0.016	IV	AB
NaC_{36}	1 Na, 36C	0.304	0.323	0.001	II	AB
NaC_{64}	1 Na, 64C	0.568	0.676	0.103	II	AB
NaC_{72}	1 Na, 72 C	0.610	0.746	0.104	II	AB
NaC_{72}	1 Na, 72 C	0.262	0.615	-0.026	IV	AB
K						
KC_6	6 K, 36 C	-0.124	-0.197	-0.251	I	AA
KC_8	2 K, 16 C	-0.134	-0.199	-0.271	I	AA
KC_{12}	3 K, 36 C	0.073	0.032	-0.076	II	AA
KC_{16}	1 K, 36 C	0.028	-0.027	-0.170	II	AA
KC_{32}	1 K, 32 C	0.055	0.064	-0.222	II	AB
KC_{32}	1 K, 32 C	0.002	0.095	-0.191	IV	AB
KC_{36}	1 K, 36C	0.012	0.062	-0.260	II	AB

KC_{64}	1 K, 64C	0.562	0.689	0.117	II	AB
KC_{72}	1 K, 72 C	0.738	0.902	0.260	II	AB
KC_{72}	1 K, 72 C	-0.013	0.367	-0.274	IV	AB
* computed with respect to AA-stacked graphite						

B) Structural deformation and binding energy contributions

Table S2. Contributions to the formation energy of AMC_x (AM = Li, Na and K).

Compound	Stacking/Stage	E_{def}, eV/f.u.	E_{bind}, eV/f.u.	E_f, eV/f.u.
AM = Li				
LiC_6	AA / I	0.090	-0.336	-0.246
LiC_8	AA / I	0.117	-0.335	-0.218
LiC_{12}	AA / II	0.167	-0.225	-0.058
LiC_{16}	AA / II	0.193	-0.232	-0.039
LiC_{32}	AB / II	0.132	-0.140	-0.008
LiC_{36}	AB / II	0.133	-0.161	-0.028
LiC_{64}	AB / II	0.131	-0.184	-0.053
LiC_{72}	AB / II	0.144	-0.222	-0.078
LiC_{32}	AB / IV	0.098	-0.098	0.0
LiC_{72}	AB / IV	0.120	-0.197	-0.077
AM = Na				
NaC_6	AA / I	0.199	-0.138	0.061
NaC_8	AA / I	0.249	-0.191	0.058
NaC_{12}	AA / II	0.293	-0.072	0.221
NaC_{16}	AA / II	0.343	-0.154	0.189
NaC_{32}	AB / II	0.475	-0.172	0.303
NaC_{36}	AB / II	0.521	-0.217	0.304
NaC_{64}	AB / II	0.681	-0.113	0.568
NaC_{72}	AB / II	0.672	-0.062	0.610
NaC_{32}	AB / IV	0.261	-0.048	0.213
NaC_{72}	AB / IV	0.511	-0.249	0.262
AM = K				
KC_6	AA / I	0.278	-0.475	-0.197
KC_8	AA / I	0.351	-0.550	-0.199
KC_{12}	AA / II	0.383	-0.351	0.032
KC_{16}	AA / II	0.464	-0.491	-0.027
KC_{32}	AB / II	0.719	-0.664	0.055
KC_{36}	AB / II	0.807	-0.795	0.012
KC_{64}	AB / II	1.362	-0.800	0.562

KC_{72}	AB / II	1.506	-0.768	0.738
KC_{32}	AB / IV	0.365	-0.363	0.002
KC_{72}	AB / IV	0.799	-0.812	-0.013

C1) Bond length and interlayer distance of AMC_x

Table S3. Comparison of the in-plane ($d^{in-plane}_{C-C}$) and the interlayer distances between graphene layers in the optimized structures of AMC_x (AM = Li, Na and K) with experimental and theoretical studies. For stage-II structures the interlayer separation is given separately for the layer with (d^{occ}_{C-C}) and without ($d^{non-occ}_{C-C}$) intercalated alkali metal. The results obtained in the present study are underlined. Color code: carbon (brown), alkali metal (green).

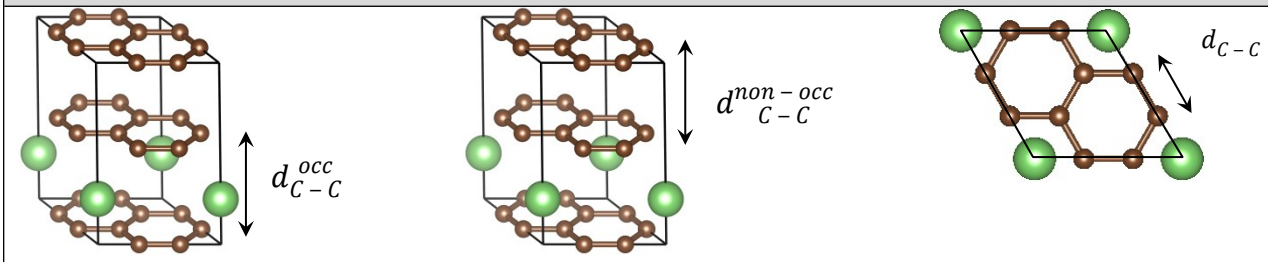

	$d^{in-plane}_{C-C}$, Å	d^{occ}_{C-C}, Å	$d^{non-occ}_{C-C}$, Å
LiC_6 (AA-I)	<u>1.439</u>, 1.440 [1], 1.492 [2]	<u>3.595</u>, 3.64 [3] , 3.697 [1], 3.706±0.01 [4], 3.705 [5] *c* = 7.40 [6]	-
LiC_8 (AA-I)	<u>1.443</u>, 1.440 [7]	<u>3.597</u> -	-
LiC_{12} (AA-II)	<u>1.429</u>, 1.429 [5], 1.431 [1], 1.431 [7], 1.429 [2]	<u>3.677</u>, d_{av} = 3.49 [3], 3.586 [1], *c* = 7.065±0.02 [4], *c* = 7.032 [2], *c* = 7.04 [6]	<u>3.305</u>, 3.27 [3]

LiC_{16} (AA-II)	1.432, 1.429 [7]	3.678 d_{av} =3.53 [3]	3.382
NaC_6 (AA-I)	1.442	4.366	-
NaC_8 (AA-I)	1.442, 1.439 [7]	4.405	-
NaC_{12} (AA-II)	1.431, 1.432 [7]	4.417	3.286
NaC_{16} (AA-II)	1.432, 1.431 [7]	4.449	3.379
KC_8 (AA-I)	1.437, 1.44 [8, 9], 1.429 [10], 1.436 [7]	5.308, 5.53 [8, 9], 5.514 [10], 5.35 [11]	-
KC_{12} (AA-II)	1.431, 1.43 [12], 1.429 [10], 1.430 [7]	5.297, 5.32 [12], 5.353 [10]	3.284
KC_{16} (AA-II)	1.430, 1.43 [9], 1.427 [10], 1.429 [7]	5.360, 5.613 [9], 5.600 [10]	3.360, 3.474 [9], 3.253 [10]

C2) Contributions to the structural deformation energy for AMC_x

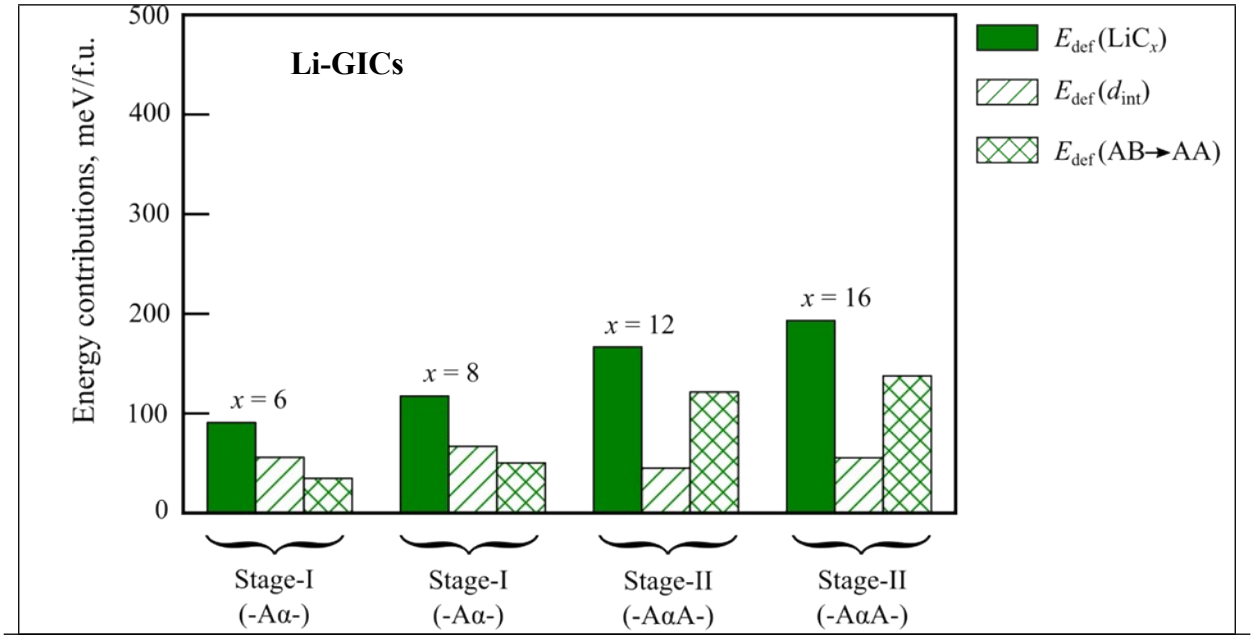

(a)

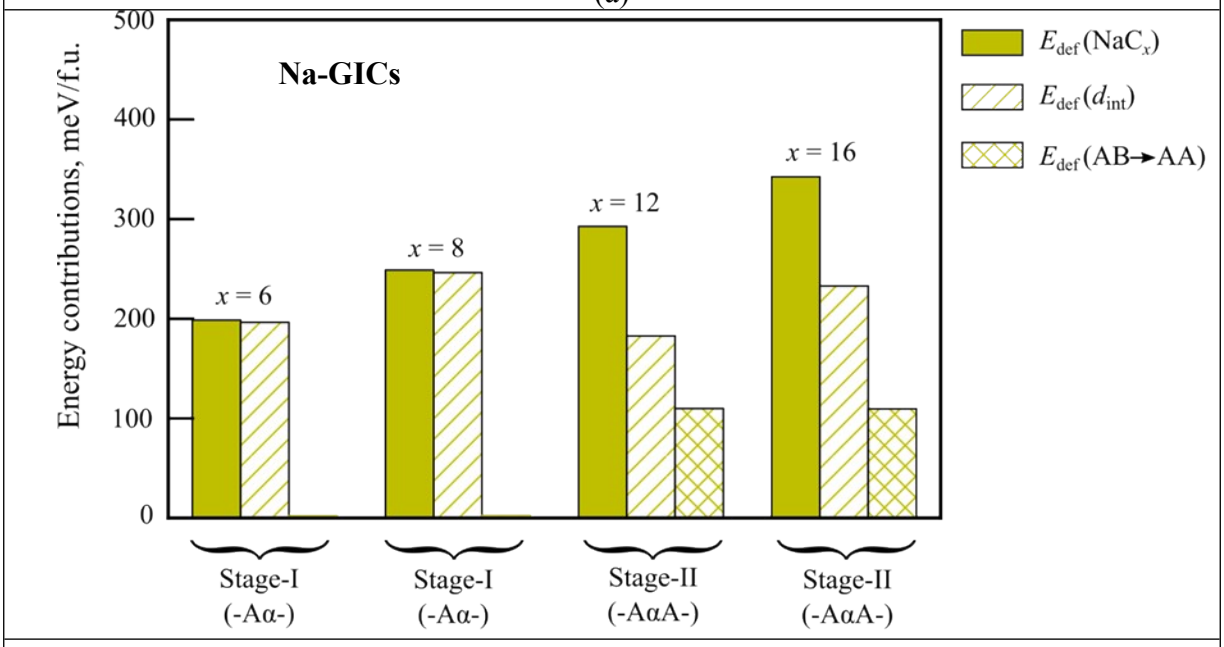

(b)

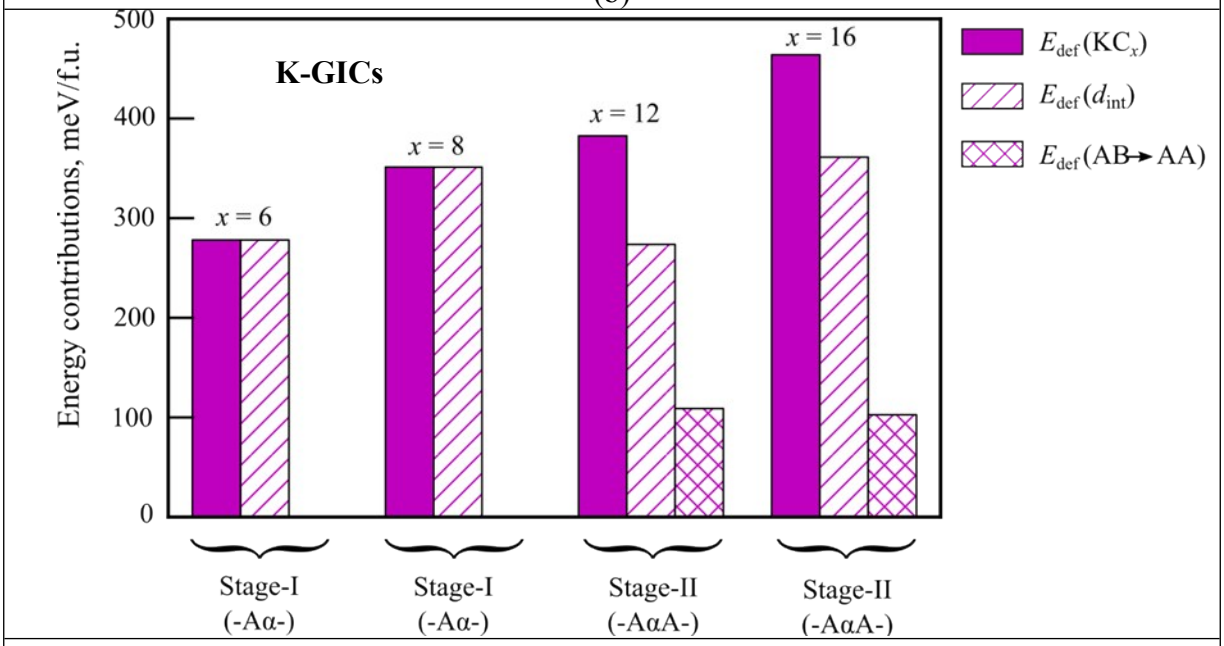

(c)

Figure S1. Energy contributions to the structural deformation energy (E_{def}) of the AMC_x (AM = Li, Na and K) for different AM-rich binary GICs compounds, possessing the AA-stacking of the graphite layers ($6 \leq x \leq 16$). The $E_{def}(d_{int})$ and $E_{def}(AB \rightarrow AA)$ contributions are defined using Eq.(5) - Eq.(6).

Table S4. Energy contributions to the structural deformation energy (E_{def}) of the AMC_x (AM = Li, Na and K) for different AM-rich binary GICs compounds, possessing the AA-stacking of the graphite layers ($6 \leq x \leq 16$). The $E_{def}(d_{int})$ and $E_{def}(AB \rightarrow AA)$ contributions are defined using Eq.(5) - Eq.(6).

Energy contributions	Li	Na	K
AMC_6			
E_{def}, meV/f.u:	91	199	278
$E_{def}(AB \rightarrow AA)$, meV/f.u	35	3	-
$E_{def}(d_{int})$, meV/f.u	56	196	278
AMC_8			
E_{def}, meV/f.u:	117	249	351
$E_{def}(AB \rightarrow AA)$, meV/f.u	50	3	-
$E_{def}(d_{int})$, meV/f.u	67	246	351
AMC_{12}			
E_{def}, meV/f.u:	167	293	383
$E_{def}(AB \rightarrow AA)$, meV/f.u	122	110	109
$E_{def}(d_{int})$, meV/f.u	45	183	274
AMC_{16}			
E_{def}, meV/f.u:	193	343	464
$E_{def}(AB \rightarrow AA)$, meV/f.u	137	110	103
$E_{def}(d_{int})$, meV/f.u	56	233	361

D1) Comparison of the cohesive and ionization energies of alkali metals

Table S5. The calculated cohesive and ionization energies of AMs (E_{ion}), as well as the difference between the ionization energy of AMs and the electron affinity of graphite (E_A = 4.76 eV), compared with other literature data.

	Li	Na	K
Cohesive energy, eV	1.60, 1.58 [13]	1.09, 1.13 [13]	0.87, 0.98 [13]
Ionization energy, eV	5.59, 5.39 [14, 15]	5.36, 5.14 [14,15]	4.46, 4.34 [14,15]

E_{ion} (AM) – E_A(Graphite), eV	0.83, 0.59 [15]	0.60, 0.34 [15]	-0.30, -0. 46 [15]

D2) van der Waals energy of AM-GICs

Table S6. The van der Waals energy contribution to the binding energy in AMC_6 (AM = Li, Na, K) is estimated by subtracting the dispersion correction part D3 of infinite (20 Å) layer separation from the dispersion correction part D3 of graphite with the interlayer distance as in the AM-GIC.

	Li	Na	K
E_{vdW}, meV	-321	-157	-67

D3) Energy contributions to the formation energy of Li-GICs

Table S7. Comparison of the energy contributions to the formation energy of stage-I LiC_6 and stage-II LiC_{12}, obtained by employing different density functionals. The contributions to the structural deformation energy are computed using Eq.(5)-(6). The binding energy contributions, see Eq.(8), are obtained using Eq.(2)-Eq.(4).

Energy contributions	PBE-D3 (BJ)	optB88-vdW	optB86b-vdW	revPBE-vdW
LiC_6				
E_{def}, eV/f.u:	0.090	0.124	0.128	0.085
E_{def}(AB→AA), eV/f.u	0.034	0.030	0.033	0.020
$E_{def}(d_{int})$, eV/f.u	0.056	0.094	0.095	0.065
E_{bind}, eV/f.u:	-0.336	-0.345	-0.343	-0.157
E_{coh}, eV	1.606	1.586	1.641	1.541
E_{ion}(Li), eV	5.587	-	5.502	5.695
E_A(Graphite), eV	4.76	4.8 [15]	4.8 [15]	4.8 [15]
[E_{ion}(Li) - E_A(Graphite)], eV	0.83	-	0.702	0.895
(E_{vdW} + $E_{elstat/cov}$), eV	-2.771	-	-2.685	-2.593
LiC_{12}				
E_{def}, eV/f.u:	0.167	0.235	0.267	0.117
E_{def}(AB→AA), eV/f.u	0.122	0.148	0.174	0.071

$E_{def}(d_{int})$, eV/f.u	0.045	0.087	0.092	0.046
$\underline{E_{bind}}$, eV/f.u:	-0.222	-0.512	-0.540	-0.236
E_{coh}, eV	1.606	1.586	1.641	1.541
E_{ion}(Li), eV	5.587	-	5.502	5.695
E_A(Graphite), eV	4.76	4.8 [15]	4.8 [15]	4.8 [15]
[E_{ion}(Li) - E_A(Graphite)], eV	0.83	-	0.702	0.895
(E_{vdW} + $E_{elstat/cov}$), eV	-2.657	-	-2.882	-2.672

REFERENCES

1. Thinius, S.; Islam, M. M.; Heitjans, P.; Bredow, T. Theoretical study of Li migration in lithium-graphite intercalation compounds with dispersion-corrected DFT methods. *J. Phys. Chem. C* **2014**, *118*, 2273−2280.
2. Missyul, A.; Bolshakov, I.; Shpanchenko, R. XRD study of phase transformations in lithiated graphite anodes by Rietveld method. *Powder Diffr.* **2017**, *32*(S1), S56−S62.
3. Hazrati, E.; de Wijs, G.A.; Brocks, G. Li intercalation in graphite: A van der Waals density functional study. *Phys. Rev. B* **2014**, *90*, 155448.
4. Guerard, D.; Herold, A. Intercalation of lithium into graphite and other carbons. *Carbon* **1975**, *13*, 337–356.
5. Billaud, D.; Henry, F.X.; Willmann, P. Dependence of the morphology of graphitic electrodes on the electrochemical intercalation of lithium ions. *J. Power Sources* **1995**, *54*, 383–388.
6. Schweidler, S.; Biasi, L.; Schiele, A.; Hartmann, P.; Brezesinski, T.; Janek, J. Volume changes of graphite anodes revisited: A combined *operando* x-ray diffraction and *in situ* pressure analysis study. *J. Phys. Chem. C* **2018**, *122*, 8829−8835.
7. Wan, W.; Wang, H. Study on the first-principles calculations of graphite intercalated by alkali metal (Li, Na, K). *Int. J. Electrochem. Sci.* **2015**, *10*, 3177–3184.
8. Ziambaras, E.; Kleis, J.; Schröder, E.; Hyldgaard, P. Potassium intercalation in graphite: A van der Waals density-functional study. *Phys. Rev. B* **2007**, ***76***, 155425.
9. Luo, W.; Wan, J.; Ozdemir, B.; Bao, W.; Chen, Y.; Dai, J.; Lin, H.; Xu, Y.; Gu, F.; Barone, V.; Hu, L. Potassium ion batteries with graphitic materials. *Nano Lett.* **2015**, *15*, 7671–7677.

10. Xu, Z.; Lv, X.; Chen, J.; Jiang, L.; Lai, Y.; Li, J. Dispersion-corrected DFT investigation on defect chemistry and potassium migration in potassium-graphite intercalation compounds for potassium ion batteries anode materials. *Carbon* **2016**, *107*, 885–894.

11. Dresselhaus, M.S.; Dresselhaus, G. Intercalation compounds of graphite. *Adv. Phys.* **1981**, *30*, 139–326.

12. Nobuhara, K.; Nakayama, H.; Nose, M.; Nakanishi, S.; Iba, H. First-principles study of alkali metal-graphite intercalation compounds, *J. Power Sources* **2013**, *243*, 585–587.

13. Brooks, H. Cohesive energy of alkali metals. *Phys. Rev.* **1953**, *91*, 1027–1028.

14. Lide, D.R. (ed), *CRC Handbook of Chemistry and Physics, 84th Edition*. CRC Press: Boca Raton, Florida, 2003.

15. Setton, R.; Bernier, P.; Lefrant, S. *Carbon Molecules and Materials*. CRC Press: Boca Raton, Florida, 2002.

16. Wang, Z.; Selbach, S.M.; Grande, T. Van der Waals density functional study of the energetics of alkali metal intercalation in graphite. *RSC Adv.* **2014**, *4*, 4069–4079.